Design and Simulation of Ultra-compact 25-Gbit/s Directly-modulated V-cavity Tunable Laser at 1310-nm Band

Lingxuan Lan, **Lin Wu**, **and Jian-Jun He**
Center for Integrated Optoelectronics
State Key Laboratory of Modern Optical Instrumentation
Department of Optical Engineering, Zhejiang University, Hangzhou 310027, China

Abstract— We design and investigate a high-speed directly-modulated tunable V-cavity laser working in the 1310-nm band. The laser is ultra-compact with a device size of only 300 μm × 200 μm. The simulation results show that 21 × 200 GHz tuning with ∼ 40 dB side-mode suppression ratio is achieved. And the simulated 3-dB bandwidth of small signal response can reach 29.9 GHz. Moreover, 10 Gbit/s and 25 Gbit/s direct modulations are demonstrated with clear eye-opening. Error-free 10-km single-mode fiber transmission is also obtained.

1. INTRODUCTION

In recent years, the spectacular increase of the traffic in both local area and access networks has led to the introduction of high-speed transmission in the 1310-nm band [1, 2]. Tunable semiconductor lasers working in this band have attracted great attention and interest. Besides their use for source sparing with the advantages of reduced inventory and cost, they are also the key components for next-generation wavelength-agile optical networks.

A variety of tunable lasers have been developed with excellent performance, such as sampled grating distributed Bragg reflector (SGDBR) lasers [3, 4], superstructure grating (SSG) DBR lasers [5, 6], digital supermode (DS) DBR lasers [7] and MEMS based lasers [8]. However, in addition to the fabrication complexities involving non-uniform gratings and multiple epitaxial regrowth, tunable lasers based on grating or MEMS structure often need many electrodes and complicated electronic circuits with multi-dimensional current control algorithms and look-up tables for wavelength tuning. Such complexities reduce the fabrication yield and operational reliability, and increase the cost as well.

To mitigate the problem, a V-cavity tunable laser structure has recently been proposed and demonstrated. It has the advantages of fabrication simplicity and compactness, and can achieve good single-mode selectivity while allowing the lasing wavelength to be tuned over a wide range. By employing this V-cavity laser structure, we have designed and investigated a high-speed directly-modulated tunable laser working in the 1310-nm band.

2. DEVICE STRUCTURE

Figure 1(a) shows the schematic diagram of the designed V-coupled cavity laser. It consists of a channel selector cavity and a reference cavity with slightly different optical path lengths, which are coupled by a reflective 2 × 2 half-wave coupler. The two coupled cavities are defined by deep trench and three electrodes are deposited within them. The gain electrode which covers the active waveguide part of the two cavities and the coupler region is used for providing optical gain and direct modulation signal. And the channel selector electrode works with the reference electrode in tuning the lasing wavelength through the Vernier effect. The detailed theory of this structure has been described in [9].

The active waveguide is based on AlGaInAs/InP multiple quantum wells (MQW) structure with five compressively strained 5.5 nm $Al_{0.172}Ga_{0.15}In_{0.678}As$ QWs sandwiched between tensilely strained 10 nm $Al_{0.295}Ga_{0.22}In_{0.485}As$ barriers. And the photoluminescence peak wavelength is about 1295 nm. By carefully designing the graded index (GRIN) layer and reducing the width of ridge waveguide to 2.5 μm, the optical field can be well confined in MQW layer while maintaining single transverse mode. In this way, the layer and waveguide structure are optimized to obtain a mode confinement factor of 0.16 for better performance. For passive waveguide, quantum well intermixing technology is used for blue shifting the bandgap, which can reduce the adverse influence of thermal-optic effect on carrier plasma-induced wavelength tuning.

The free spectral ranges of the channel selector cavity and the reference cavity are designed to be 190 GHz (i.e., 220 μm cavity length) and 220 GHz (i.e., 210 μm cavity length), respectively. By optimizing the normalized cross-coupling coefficient $\chi = |C_{12}|^2 \cdot (|C_{12}|^2 + |C_{22}|^2)^{-1}$ to 0.025, a

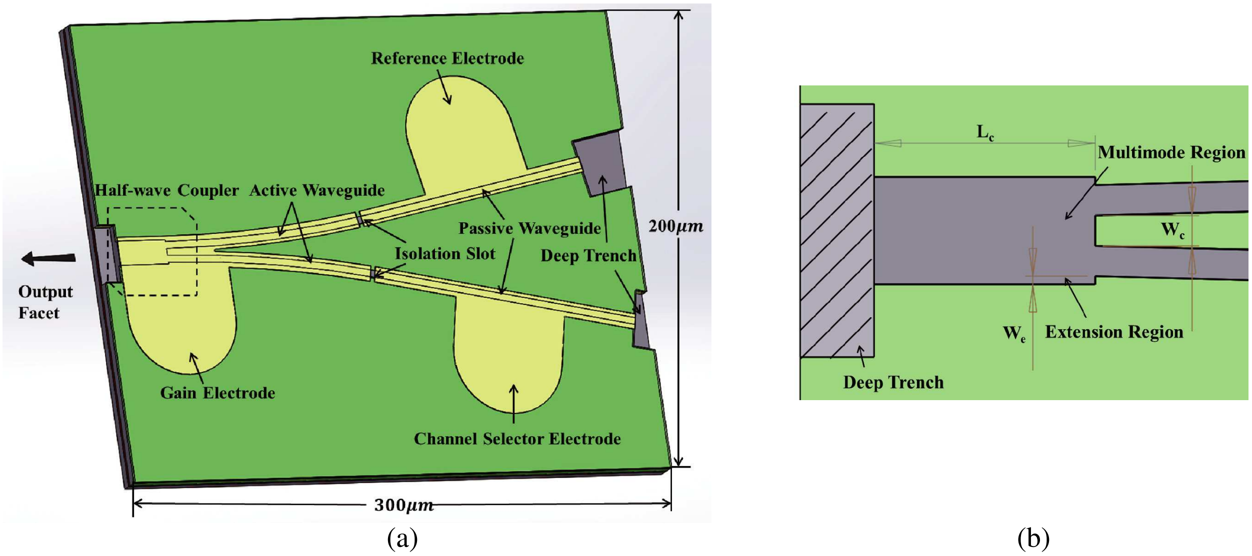

Figure 1: Schematic diagram of (a) the V-cavity laser and (b) the half-wave coupler.

large threshold gain difference of $6.95\,\mathrm{cm}^{-1}$ is obtained. To achieve this target χ with a relative phase $\phi = m\pi$ $(m = 0, \pm1, \pm2, \ldots)$ as well as reduce excess loss which can be calculated as $\varepsilon = -10\log_{10}(|C_{11}|^2 + |C_{12}|^2 + 2|C_{11}||C_{12}|\cos(\varphi)|)$, two extension regions are added to the half-wave coupler, as shown in Figure 1(b). Through 3D parameters scanning of the width of the extension regions W_e, the width of the gap W_c and the length of the multimode coupling region L_c, the optimal parameters can be found, which are $W_e = 0.5\,\mu\mathrm{m}$, $W_c = 2.75\,\mu\mathrm{m}$ and $L_c = 26.5\,\mu\mathrm{m}$. From the overall structure perspective, the V-cavity laser is ultra-compact with a device size of only $300\,\mu\mathrm{m} \times 200\,\mu\mathrm{m}$.

3. STATIC AND DYNAMIC CHARACTERISTICS

Static and dynamic simulations for tunable lasers are important for reducing the R&D costs and improving the performance efficiently. The time-domain traveling-wave (TDTW) method is commonly used to model various characteristics of tunable lasers [10, 11]. In this paper, an advanced TDTW implementation called PICWave is used to perform simulations of our device. The details of the theoretical model can be found in [12].

We first calculate the output power emitted from the channel selector cavity facet and the junction voltage as a function of the injected current on the gain electrode while the channel selector electrode and the reference electrode are biased at 9.7 and 26 mA, respectively. As shown in Figure 2, turn-on voltage is about 1 V and threshold current is 23.6 mA. No kinks are observed on the L-I-V curves.

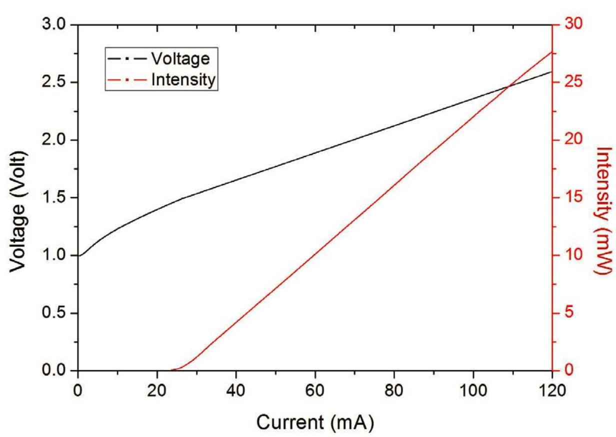

Figure 2: The output power and the voltage as a function of injection current.

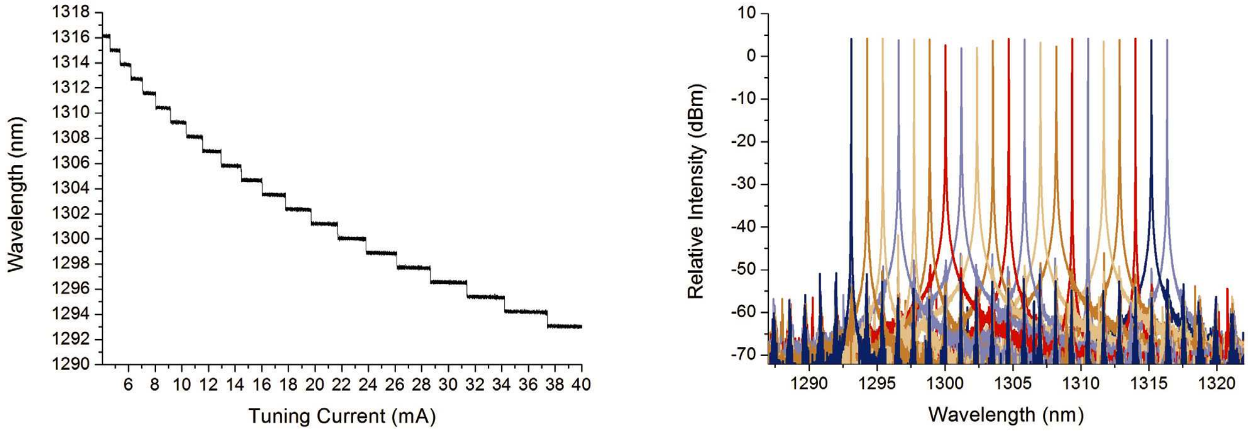

(a) (b)

Figure 3: (a) Simulated tuning characteristics and (b) superimposed 21 channels laser spectra.

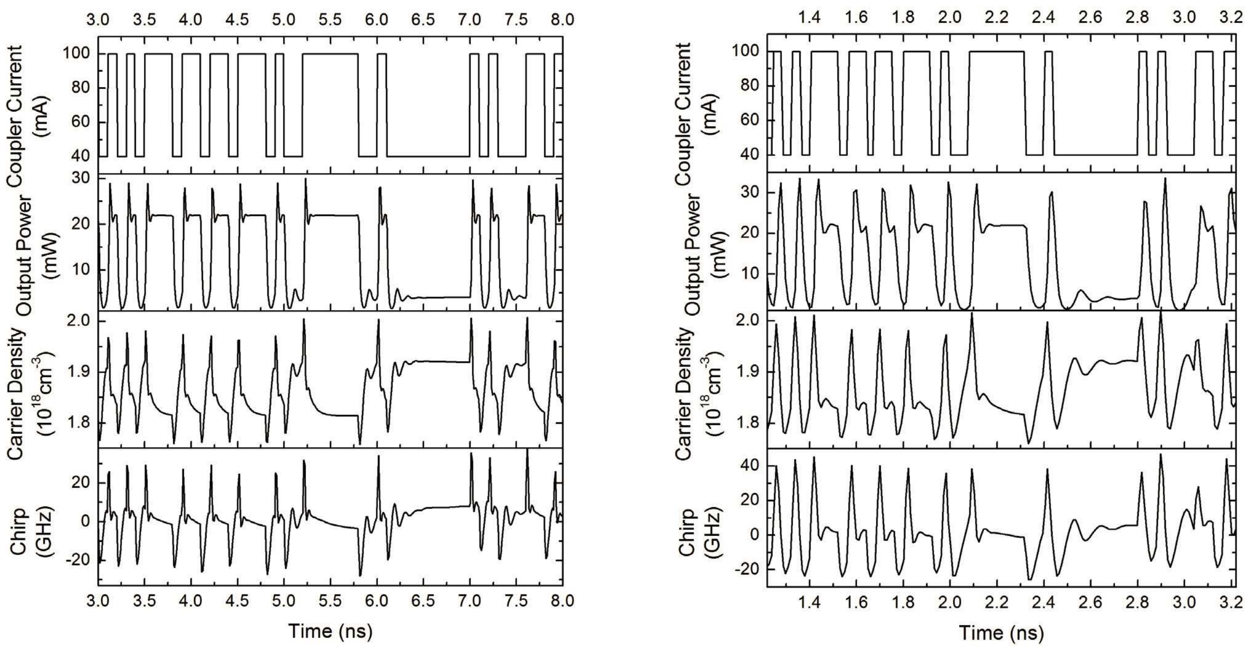

(a) (b)

Figure 4: Time response of large signal (a) 10 Gbit/s and (b) 25 Gbit/s direct intensity modulation.

To simulate the single electrode controlled discrete tuning characteristics of the V-cavity laser, we set the current on the gain electrode and the reference electrode fixed at 70 and 26 mA, respectively. As shown in Figure 3(a), when the current on the channel selector electrode increase from 4 mA to 40 mA, wavelength switching of 21 consecutive channels with 200 GHz channel spacing from 1293 to 1316.2 nm is achieved. The corresponding superimposed spectra are shown in Figure 3(b), with about 40 dB side-mode suppression ratio.

Small signal response simulation is carried out by injecting a current impulse to the gain electrode, and then using the FFT algorithm to analyze the frequency spectrum of the received electrical power. The simulated 3-dB bandwidth is 29.9 GHz when the gain electrode is biased at 70 mA, showing good modulation characteristic.

In order to achieve large extinction ratio in direct intensity modulation, large bias current and modulation depth of the RF signal are needed. However, this would increase the wavelength chirp in return. Thus, a compromise between the extinction ratio and the chirp is made. Bias current and modulation depth on the gain electrode are set to 70 and 30 mA, which corresponds to 40 mA for "0" and 100 mA for "1". Then, 10 Gbit/s and 25 Gbit/s pseudo-random NRZ current signals are injected into the gain electrode, the time response of output power, the carrier density, and the chirp are simulated through the TDTW model, as shown in Figure 4. From this figure, we can see that as the injected current increases, the output power increases with an obvious overshoot while this overshoot can be suppressed by a low-pass filter in practice. Even though the transient chirp of 25 Gbit/s operation at the rising edge increases about 16 GHz in contrast to 10 Gbit/s operation, the transient chirp at the falling edge and adiabatic chirp don't show any degradation.

A 0.5-μs-long 10 Gbit/s and a 0.3-μs-long 25 Gbit/s 32-bit pseudorandom NRZ sequences are used to generate the eye diagrams of the direct intensity modulations, which are shown in Figure 5. Both eyes are clearly open with an extinction ratio of over 8 dB. Then we use OptiSystem Software to simulate the bit error rate (BER) performance for 25 Gbit/s operation after 10-km single-mode fiber transmission. When received power is -10.97 dBm, the BER of received signal is about 3.1×10^{-14}, which shows error-free ($\text{BER} < 10^{-12}$) operation is possible.

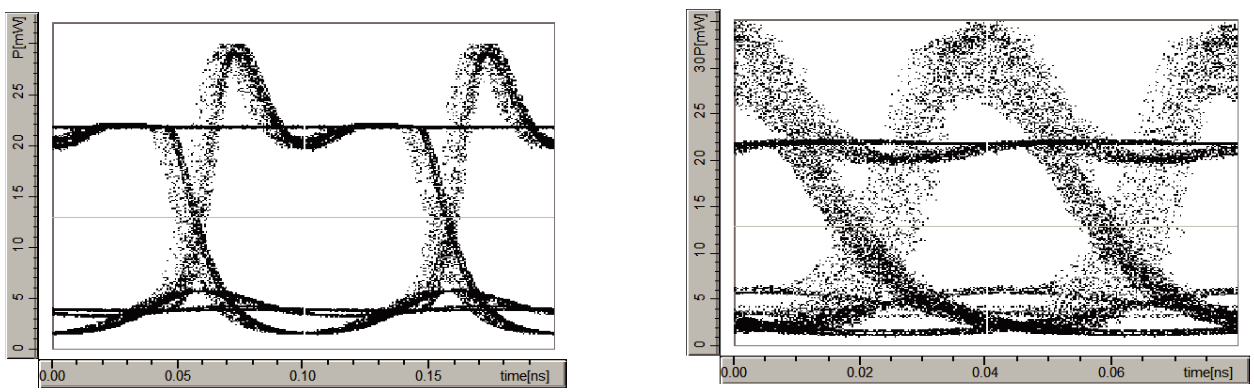

(a) (b)

Figure 5: Eye diagram of (a) 10 Gbit/s and (b) 25 Gbit/s direct intensity modulation.

4. CONCLUSION

We have presented the design and simulations of a high-speed directly-modulated tunable V-cavity laser working in the 1310-nm band with an ultra-compact size of 300 μm × 200 μm. The time-domain traveling-wave model is employed to investigate the static and dynamic characteristics. 21×200 GHz tuning with ~ 40 dB side-mode suppression ratio is achieved. The simulated 3-dB bandwidth is 29.9 GHz when the gain electrode is biased at 70 mA and extinction ratio of 10 Gbit/s and 25 Gbit/s direct modulations are both over 8 dB. Error-free 10-km single-mode fiber transmission is also obtained. The proposed device is a promising candidate for light source of wavelength-agile access and data center networks.

ACKNOWLEDGMENT

This work was supported by the National High-Tech R&D Program of China (grant 2013AA014401) and the National Natural Science Foundation of China (grant 61377038).

REFERENCES

1. Kapon, E. and A. Sirbu, "Long-wavelength VCSELs: Power-efficient answer," *Nature Photonics*, Vol. 3, No. 1, 27–29, 2009.
2. Ingham, J. D., M. Webster, A. Wonfor, et al., "Wide-frequency-range operation of a high-linearity uncooled DFB laser for next-generation radio-over-fiber," *Optical Fiber Communication Conference*, Optical Society of America, FO3, 2003.
3. Mason, B., G. A. Fish, S. P. Den Baars, et al., "Widely tunable sampled grating DBR laser with integrated electroabsorption modulator," *IEEE Photonics Technology Letters*, Vol. 11, No. 6, 638–640, 1999.
4. Coldren, L. A., "Monolithic tunable diode lasers," *IEEE Journal of Selected Topics in Quantum Electronics*, Vol. 6, No. 6, 988–999, 2000.
5. Tohmori, Y., Y. Yoshikuni, H. Ishii, et al., "Broad-range wavelength-tunable superstructure grating (SSG) DBR lasers," *IEEE Journal of Quantum Electronics*, Vol. 29, No. 6, 1817–1823, 1993.

6. Ishii, H., F. Kano, Y. Tohmori, et al., "Narrow spectral linewidth under wavelength tuning in thermally tunable super-structure-grating (SSG) DBR lasers," *IEEE Journal of Selected Topics in Quantum Electronics*, Vol. 1, No. 2, 401–407, 1995.
7. Ward, A. J., D. J. Robbins, G. Busico, et al., "Widely tunable DS-DBR laser with monolithically integrated SOA: design and performance," *IEEE Journal of Selected Topics in Quantum Electronics*, Vol. 11, No. 1, 149–156, 2005.
8. Berger, J. D., Y. Zhang, J. D. Grade, et al., "Widely tunable external cavity diode laser using a MEMS electrostatic rotary actuator," *IEEE Advanced Semiconductor Lasers and Applications, Digest of the LEOS Summer Topica*, 2, 2001.
9. He, J. J. and D. Liu, "Wavelength switchable semiconductor laser using half-wave V-coupled cavities," *Optics Express*, Vol. 16, No. 6, 3896–3911, 2008.
10. Dong, L., R. Zhang, D. Wang, et al., "Modeling widely tunable sampled-grating DBR lasers using traveling-wave model with digital filter approach," *Journal of Lightwave Technology*, Vol. 27, No. 15, 3181–3188, 2009.
11. Zhi, J., H. Zhu, D. Liu, et al., "Travelling wave analysis on high-speed performance of Q-modulated distributed feedback laser," *Optics Express*, Vol. 20, No. 3, 2277–2289, 2012.
12. Wu, L., J. J. He, and D. Gallagher, "Modeling of widely tunable V-cavity semiconductor laser using time-domain traveling-wave method," *JOSA B*, Vol. 32, No. 2, 309–317, 2015.